Published in final edited form as:
J Androl. 2011 ; 32(4): 444–463. doi:10.2164/jandrol.110.010694.

Alterations in the Testis and Epididymis Associated with Loss of Function of the Cystatin Related Epididymal Spermatogenic (CRES) Protein*

Adam D. Parent[1], **Gail A. Cornwall**[2], **Lauren Y. Liu**[1], **Charles E. Smith**[3], and **Louis Hermo**[1]

[1]Department of Anatomy and Cell Biology, McGill University, 3640 University St., Montreal, Quebec, H3A 2B2

[2]Department of Cell Biology and Biochemistry, Texas Tech University Health Sciences Center, 3601 4th Street, Lubbock, Texas 79430, USA

[3]Faculté de Médicine Dentaire, Université de Montréal, Pavillon Roger-Gaudry (A-221), 2900 Blvd. Edouard-Montpetit, Montreal, Quebec, H3T 1J4, and Faculty of Dentistry, McGill University, 3640 University St., Montreal, Quebec H3A 2B2

Abstract

CRES (*Cst8*) is a member of the cystatin superfamily of cysteine protease inhibitors. It differs from typical cystatins because it lacks consensus sites for cysteine protease inhibition and exhibits reproductive specific expression. In the present study, we examined CRES within the testis, efferent ducts and epididymis of normal mice by light microscope immunolocalization. Alterations to these tissues in male mice lacking the *Cst8* gene ($Cst8^{-/-}$) were also characterized by histomorphometry and electron microscopy. In the normal testis, CRES was localized exclusively in mid and late elongating spermatids. In the efferent ducts, CRES was localized to the apical region of the epithelial cells suggestive of localization in the endosomes. In the initial segment of the epididymis, principal cells showed supranuclear and luminal reactions. In the cauda region, CRES was present exclusively as aggregates in the lumen and was detected in clear cells. Compared to wildtype mice ($Cst8^{+/+}$) in older (10–12 month age) $Cst8^{-/-}$ mice, modest but statistically significant reductions were detected in tubular, epithelial and/or luminal profile areas in the testis and epididymis. By electron microscopy, some $Cst8^{-/-}$ tubules in the testis were normal in appearance but others showed a vacuolated seminiferous epithelium, degenerating germ cells and alterations to ectoplasmic specializations. In the epididymal lumen, abnormally shaped sperm heads and tails were noted along with immature germ cells. In addition, principal cells contained numerous large irregularly shaped lysosomes suggestive of disrupted lysosomal functions. In both the testis and epididymis, however, these abnormalities were not apparent in younger mice (4 months of age) but only in the older (10–12 month old) $Cst8^{-/-}$ mice. These findings suggest that the altered testicular and epididymal histology reflects a cumulative effect of the loss of CRES and support a role for CRES for maintaining the normal integrity and function of the testis and epididymis.

Keywords

spermatids; principal cells; efferent ducts; lysosomes; clear cells; cystatins

*This work was funded by CIHR (LH) and NIH HD33903, HD56182 (GAC)

Correspondence: Gail A. Cornwall, Ph.D., Department of Cell Biology and Biochemistry, Texas Tech University Health Sciences Center, 3601 4th Street, Lubbock, Texas 79430, USA, Phone: 806.743.2700 x246, gail.cornwall@ttuhsc.edu.

Introduction

In the testis, spermatogenesis is the process whereby spermatogonia divide giving rise to spermatocytes which undergo meiotic divisions to produce haploid spermatids (Leblond and Clermont, 1952; Clermont, 1972). The latter undergo a remarkable metamorphosis during their development, termed spermiogenesis, in which the round spermatids evolve into elongating spermatids that eventually are released as spermatozoa into the seminiferous tubular lumen. In the mouse, 16 steps of spermiogenesis have been defined (Oakberg, 1956) and during the last half of this process, there is significant protein synthesis in spermatids that helps facilitate the incredible changes in spermatid morphology (De Kretser and Kerr, 1988; Clermont et al, 1993; Hecht, 1998; Hermo et al, 2010). Other important processes that occur during spermiogenesis include formation of the acrosome, chromatoid body, flagellum and chromatin condensation (De Kretser and Kerr, 1988; Clermont et al, 1993; Parvinen, 2005; Kierszenbaum et al, 2007; Nagamori and Sassone-Corsi, 2008; Hermo et al, 2010).

Once spermatozoa are released from the seminiferous epithelium, they converge upon the efferent ducts, where nonciliated cells are engaged in removing luminal fluids and proteins in an effort to concentrate spermatozoa as they enter the initial segment of the epididymis (Crabo, 1965; Robaire and Hermo, 1988; Hermo et al, 1994; Ilio and Hess, 1994; Hess, 2000; 2002; Hermo and Robaire, 2002). Upon exiting the efferent ducts, the immature spermatozoa enter the epididymis, a highly coiled duct lined by an epithelium well known for its cell type and regional specificity in structure and function. Principal cells are highly secretory in nature, while clear cells are endocytic, and in combination with the narrow and basal cells help regulate luminal microenvironments conducive for sperm maturation (Hamilton, 1975; Orgebin-Crist et al, 1975; Robaire and Hermo, 1988; Hermo et al, 1994; Cornwall et al, 2002; Robaire et al, 2006; Cornwall, 2009).

CRES (Cystatin Related Epididymal Spermatogenic) or cystatin 8 (*Cst8*) is the defining member of a reproductive subgroup within the family 2 cystatins in the cystatin superfamily of cysteine protease inhibitors (Cornwall et al, 1999, Cornwall and Hsia,2003). There are eight CRES subgroup family members all characterized by their lack of consensus sites for cysteine protease inhibition and reproductive-specific expression. Although CRES contains the typical C-terminal PW loop and distinct N-terminus, it lacks the highly conserved glutamine-valine-glycine (Q-X-V-X-G) pentamer present in typical cystatins (Cornwall et al, 1992). *In vitro* CRES inhibited the serine protease prohormone convertase 2, which processes precursor hormones/proteins into their mature and active forms. This suggests a function for CRES that is distinctly different from the cysteine protease inhibitor activity associated with most cystatins (Cornwall et al, 2003; 2007).

CRES is of particular interest since it is found mainly in the testis and epididymis (Cornwall et al, 1992), as well as the gonadotropes of the anterior pituitary (Sutton et al, 1999; Sutton-Walsh et al, 2006) and in the corpus luteum (Hsia and Cornwall, 2003; Hsia et al, 2005). In the testis, CRES localizes to the cytoplasmic region of spermatids at specific steps in their development, while in the epididymis, CRES is synthesized and secreted by the principal cells primarily within the initial segment (Cornwall and Hann, 1995). CRES has also been shown to be associated with the acrosomes of testicular and epididymal spermatozoa in mice and within the equatorial segment of human ejaculated spermatozoa (Syntin and Cornwall, 1999; Wassler et al, 2002).

Studies focused on disrupting cystatin genes have shown that mice lacking cystatin B (*CstB*) develop familial epilepsy (Pennacchio et al, 1996) while mice lacking the cystatin M/E gene demonstrate abnormalities in epidermal cornification (Zeeuwen et al, 2004). Mice lacking the testatin gene ($Cst9^{-/-}$), a member of the CRES subgroup that is expressed in the

developing testis and adult Sertoli cells, showed no obvious reproductive phenotype (Tohonen et al., 1998; Tohonen et al., 2005). However, except for breeding experiments, these studies primarily focused on examination of *Cst9*$^{-/-}$ in fetal mice and a detailed analysis of the adult was not carried out. In contrast to *Cst9*, male mice lacking the CRES gene (*Cst8*$^{-/-}$) demonstrated a fertility defect in vitro as shown by reduced ability of *Cst8*$^{-/-}$ spermatozoa to fertilize cumulus oocyte complexes and to bind to the zona pellucida. Further analysis suggested the defect resided in the ability of the spermatozoa to undergo capacitation since compared to wildtype, *Cst8*$^{-/-}$ spermatozoa showed reduced protein tyrosine phosphorylation and ability to acrosome react in the presence of progesterone (Chau and Cornwall, in press). Because exposure of *Cst8*$^{-/-}$ spermatozoa to dibutyryl cAMP and isobutylmethylxanthine rescued the fertility defect in vitro including the levels of protein tyrosine phosphorylation, this suggested that the loss of CRES may result in altered cell signaling during capacitation.

Other pathologies associated with cystatins include hereditary cystatin c amyloid angiopathy, which results from a mutation in the human cystatin C gene (*Cst3*) and accompanying expression of a highly amyloidogenic cystatin C protein (Ghiso et al, 1986). Indeed, it has also been noted that CRES has a high propensity to self-aggregate *in vitro* implying the potential for CRES to undergo amyloidogenesis *in vivo* (von Horsten et al, 2007). Although preliminary biochemical studies suggest the presence of CRES amyloid within the epididymal lumen, the functional significance of these structures has yet to be determined (Cornwall, personal communication). The presence of amyloid in the testis and epididymis has been implicated as a factor contributing to infertility (Nistal et al, 1989; Haimov-Kochman et al, 2001).

The main purpose of this study was to undertake a more detailed analyses of the distribution of CRES protein within the male tract of adult mice, using improved methods of fixation and visualization for light microscope (LM) immunocytochemistry, and to characterize abnormalities, both quantitatively using histomorphometry and qualitatively by electron microscopy, occurring in the testis, efferent ducts and epididymis of *Cst8*$^{-/-}$ mice as compared to wild type mice.

Materials and Methods

Tissue Preparation of Cst8$^{+/+}$ and Cst8$^{-/-}$ mice: Light and Electron Microscopy

Cst8$^{+/+}$ and *Cst8*$^{-/-}$ male mice were bred at Texas Tech University Health Sciences Center, Lubbock, TX and then shipped live to Montreal where they were acclimatized for a few days before being used for experiments. In Texas and Montreal, the mice were maintained on a 12hr light/12hr dark cycle, handled and eventually euthanized in accordance with NIH guidelines for the care and use of experimental animals. The *Cst8*$^{-/-}$ mice were generated through targeted disruption of the *Cst8* gene by InGenious Targeting Laboratory, Inc (Stony Brook, NY) using a neomycin cassette in a classic homologous recombination strategy. The *Cst8*$^{-/-}$ mice were generated on a 129 SvEv background and then backcrossed with C57BL6/J for several generations. Northern and western blot analyses were performed to confirm absence of *Cst8* mRNA and protein expression (Chau and Cornwall, in press).

Six *Cst8*$^{+/+}$ and six *Cst8*$^{-/-}$ mice were used for light and electron microscopy, as well as for quantitative analyses. Within each group (*Cst8*$^{+/+}$/*Cst8*$^{-/-}$), 3 mice were 4 months old and 3 mice were 10–12 months old. Mice were anesthetized by intraperitoneal injection of sodium pentobarbital (Somnitol, MTC Pharmaceuticals, Hamilton, ON). Blood vessels, efferent ducts and the epididymis on the right side of the animal were clamped with a haemostat, excised away from the testis and immersed in Bouin's or zinc fixative (BD Biosciences, Mississauga, ON; Beckstead, 1994; Hermo et al, 2008). The tissues were dehydrated

through a graded series of ethanol and embedded in paraffin. Sections were cut at 5 μm and placed on coated glass slides. The epididymides from all mice were oriented along their long axes to reveal the 4 major regions in every section (Hermo et al, 1991).

Once removal of reproductive tissues from the right side of an animal was completed, each mouse was perfused via the heart and descending aorta with 2.5% glutaraldehyde in 0.1M sodium cacodylate buffer, pH 7.4 containing 0.05% calcium chloride. After 10 minutes, the testis, efferent ducts, and samples of the 4 major regions of the epididymis were excised on the left side and cut into small 1 mm^3 blocks. The samples were placed in fresh fixative on ice for several hours and then washed overnight at 4°C in 0.1M sodium cacodylate buffer, pH 7.4. The next day, samples were washed 3 times for 10 minutes each in cacodylate buffer and immersed for 2 hrs in a solution containing 1% osmium tetroxide and 1.5% potassium ferrocyanide. The tissues were dehydrated in a graded series of acetone and embedded in Epon812 substitute (Mecalab Ltd., Montreal, QC). Thin sections of selected regions of the testis and epididymis were cut with a diamond knife and mounted on copper grids. The grids were stained for 5 minutes with uranyl acetate and 3 minutes with lead citrate and examined in a FEI Tecnai 12 120kV Transmission Electron Microscope (TEM).

Light Microscope Immunocytochemistry

Adult Sprague Dawley® rats and C57BL/6 mice were purchased from Charles River Laboratories Canada (St. Constant, QC) and housed and euthanized locally at a McGill University Animal Facility according to guidelines monitored by the McGill University Animal Care Committee. Samples of testis, efferent ducts and epididymis were obtained from these animals following either immersion or perfusion fixation with Bouin's or zinc fixative. All samples were processed for embedding in paraffin (n=4 for both rats and mice; ages ranging between 3 and 6 months). Sections (5 μm) of these tissues were deparaffinized in Citrisolv and rehydrated in a series of graded ethanol. The sections were washed for 5 minutes in phosphate buffered saline (PBS) and the slides were immersed in a 7.1 mM citrate buffer (pH 6.0) and microwaved at full power for 3 minutes followed by 7 minutes at 60% power. The slides were cooled to room temperature. The sections were then immersed in a peroxidase blocker solution containing 0.03% hydrogen peroxide and 0.031M sodium azide (Dako Canada Inc., Mississauga, ON) and incubated at 37°C for 90 minutes with affinity purified polyclonal rabbit anti-CRES antibody (10 μg/ml) in 50 mM Tris-Cl, pH 7.4 containing 1% BSA (Sigma A7511). This antibody is specific and exhibits no immunoreactivity when preincubated with excess CRES protein (Cornwall and Hann, 1995) as was done in this study at a 10:1 (protein:antibody) molar ratio for negative controls. The CRES protein and antibody were incubated together for 30 minutes at room temperature in 1% BSA in 50 mM Tris-Cl, pH 7.4 prior to addition to the slides. The sections were washed six times for 5 minutes each with 0.1% Tween 20 in Tris buffer (TBST; see next section) and incubated for 30 minutes at 37°C with a secondary anti-rabbit polymer-HRP (horseradish peroxidase) solution (Dako Canada Inc., Mississauga, ON) used directly from the kit. The sections were washed in TBST (5 times for 2 min each) and treated with a 2% 3,3-diaminobenzidine (DAB) solution (Dako Canada Inc., Mississauga, ON). The sections were counterstained with methylene blue, dehydrated in a series of graded ethanol and Citisolv, and mounted with cover slips using permount.

Fluorescence Microscopy

Sections of zinc fixed rats and mice testes, efferent ducts and epididymis were deparaffinized in hexane, rehydrated in a graded series of ethanol and washed with 50 mM Tris buffer, pH 7.4 containing 0.9% NaCl (TBS). The sections were microwaved in citrate buffer as described above for antigen retrieval, cooled and washed in TBS. The sections were washed an additional 6 times for 2 minutes each in 50 mM Tris buffer, pH 7.4

containing 1.8% NaCl and 0.1% Tween 20 (TBST). The sections were blocked for 30 minutes at room temperature with 2% skim milk in TBST and incubated for 3 hours at room temperature with polyclonal rabbit anti-mouse CRES antibody (12.5 μg/ml) in 50 mM Tris-Cl, pH 7.4 containing 1% BSA. The sections were washed 6 times for 2 minutes each with TBST, blocked a second time for 20 minutes with 2% skim milk in TBST and incubated for 30 minutes at room temperature with a secondary goat anti-rabbit antibody (4 μg/ml) conjugated to Alexa-594 (Invitrogen™, Burlington, ON) and diluted in 1%BSA/50 mM Tris-Cl pH 7.4. The sections were washed 5 times for 2 minutes each with TBST followed by 5 washes for 2 minutes each with TBS. Nuclei were stained with 300 nM DAPI in TBS (4′, 6-diamidino-2-phenylindole, dihydrochloride; Invitrogen™, Burlington, ON) for 2 minutes at room temperature. The sections were rinsed in TBS and mounted with cover slips using ProLong® Gold antifade reagent (Invitrogen™, Burlington, ON).

Quantitative Analyses of Tubule Profile Areas

A total of 6 *Cst8*$^{+/+}$ and 6 *Cst8*$^{-/-}$ mice equally divided at 4 and 10–12 months of age were used for quantitative analyses. Measurements of testicular and epididymal tubular profile areas in section were done using Version 4.5 of the Zeiss Axiovision LE Imaging Software (Carl Zeiss Canada Ltd., Toronto ON). Digital images of hemotoxylin and eosin (H&E) stained tubules were acquired with a Lumenera Infinity 1 camera (Lumenera Corp., Ottawa, ON). Sites for sampling seminiferous tubules, efferent ducts and epididymal tubules were chosen in a consistent, but randomized fashion as mapped on a Cartesian plane. Selected tubules were outlined once to define their outer profile areas and then a second time to delineate their inner luminal profile areas in square micrometers. From these two measurements, epithelial profile areas were deduced by subtraction (outer tubule profile area – inner luminal area = area occupied by epithelium)

Statistical analyses including Shapiro-Wilk's tests for normality, Grubb's tests for detecting outliers, ANOVA with Tukey-honest significant difference tests (for normally distributed data) or Mann-Whitney tests (alternative nonparametric test) were done using Version 8 of Statistica for Windows (Statsoft, Inc., Tulsa, OK). In all cases, p values less than 0.05 were considered significant. Graphs of results from area measurements were plotted as means ± 95% confidence intervals.

Results

CRES localization in the testis

Particular emphasis was placed in the light microscopic studies on the use of a zinc fixative first introduced by Beckstead in 1994. Proteins do not chemically cross-link with this fixative allowing for retention of good antigenicity (Benavides et al, 2006; Lykidis et al, 2007; Hermo et al, 2008). In addition, zinc fixed tissues show less autofluorescence compared to those fixed in Bouin's fluid allowing for better imaging. However, to validate results obtained with the zinc fixative method, a conventional LM immunoperoxidase immunolocalization method with Bouin's was also employed as a positive control.

Similar immunolocalization results in adult mouse testis were obtained by both LM immunofluorescence (zinc fixative) and by immunoperoxidase (Bouin's fixative) methods. In all cases, the anti-mouse CRES antibody localized exclusively to spermatids according to specific steps of spermiogenesis (Figure 1a–f). Immunoreactions first appeared in step 7 round spermatids and gradually intensified up to step 12 elongating spermatids and remained strong until spermiation at step 16 (Figure 1b–d). Immunoreactions were also seen in forming residual bodies at stage VIII–IX and were present as spermatids descended into the Sertoli cell cytoplasm at stages X–XI. The cytoplasmic droplets of elongating step 16

spermatids were not immunoreactive as they formed at stage VIII of the cycle (Figure 1c,d). Negative controls which included sections incubated in the absence of primary antibody or with antibody pretreated with antigen (block) demonstrated the specificity of the CRES antibody since no immunoreactivity was detected over the entire epithelium of the testis or epididymis (insets of Figure 1c and e).

CRES localization in the efferent ducts

Intense uniform immunoreactions were seen near the apices of ciliated and nonciliated epithelial cells in most tubules in the mouse (Figure 2a,b). At higher magnification, the reactions were punctate in nature in nonciliated cells, suggestive of localization in endosomes, which are prominent in the apical region of these cells (Figure 2b). The lumen was devoid of reaction product as were spermatozoa. Occasional but not consistent CRES immunoreactions appeared over microvilli or cilia of cells lining the duct (Figure 2a,b).

CRES localization in the epididymis

Immunoreactions for CRES were very strong in the mouse proximal initial segment, with a prominent and uniform staining over the apical region of principal cells and a supranuclear ribbon-like reaction (Figure 2c). In Bouin's-fixed tissues, a distinct supranuclear reaction was also observed over some principal cells along with an apical reaction (Figure 2d). In addition, there were strong reactions within the lumen of the epididymis (Figure 2c,d).

An epithelial reaction was absent in the distal initial segment except for some apical localization in the principal cells and in the lumen. In the caput and more distal regions, principal cells were not reactive (Figure 2e,f), whereas discrete foci of CRES immunoreactivity of different shapes and sizes were found in the lumen (Figure 2e,f). Such foci were also evident in the initial segment but became prominent in the corpus, with increasing numbers evident in the cauda region, where some aggregates appeared to hover near the microvillar border of principal cells (Figure 2f). In the cauda region, an intense immunoreaction for CRES was also seen in some clear cells (Figure 2f). CRES immunolocalization was also examined in the adult rat testis, efferent ducts, and epididymis and the results were similar to that described in the mouse (data not shown).

Morphometric analyses of $Cst8^{+/+}$ and $Cst8^{-/-}$ tissues

The testis, efferent ducts and epididymis of $Cst8^{+/+}$ and $Cst8^{-/-}$ mice were stained with hematoxylin and eosin and qualitatively analyzed. These studies suggested that the tubular and epithelial areas of $Cst8^{-/-}$ mice were smaller than their wildtype counterparts (Figure 3a–f) and hence morphometric analyses were performed. The tubule, epithelium, and luminal areas were examined for $Cst8^{+/+}$ (wildtype, WT), and $Cst8^{-/-}$ (knockout, KO) mice at 4 months and 10–12 months of age.

In the testis, without taking into account the different stages of the cycle of the seminiferous epithelium, the 10–12 month old $Cst8^{-/-}$ mice showed modest but significantly smaller tubular, epithelial, and luminal areas compared to wild type mice (Figure 4a). The 4 month old $Cst8^{-/-}$ mice also showed a significant decrease in testicular tubular, epithelial, and luminal areas but the effect was not as dramatic as that observed in the older mice (data not shown). Since the different stages of the seminiferous epithelium are associated with different sizes (Wing and Christensen, 1982), studies were carried out to quantitatively examine stage specific differences between 10–12 month old $Cst8^{+/+}$ and $Cst8^{-/-}$ mice. Indeed, the epithelium is known to be largest at stage V and smallest at stage XI and thus these two stages were chosen to normalize the data in order to determine if differences exist within these specific stages in $Cst8^{+/+}$ and $Cst8^{-/-}$ mice. This analysis indicated that some of the previous differences noted were related to stage-specific size effects. For example, at

stage V of the cycle, *Cst8*$^{-/-}$ mice had significantly smaller tubular and epithelial areas whereas at stage XI only luminal areas were significantly smaller in *Cst8*$^{-/-}$ mice (Figure 4b).

In the efferent ducts (ED), no data were generated for the 4 month old *Cst8* mice. However, in the 10–12 month old *Cst8*$^{-/-}$ mice, the efferent duct tubule and luminal areas were significantly decreased compared to that in the wildtype mice (Figure 4c). However, the epithelium did not show any difference when compared to wildtype mice.

In the epididymis, results from the area measurements were variable (Figure 4d,e,f) except in the proximal initial segment where the 10–12 month old *Cst8*$^{-/-}$ mice exhibited large decreases in tubular, epithelial, and luminal areas compared to that in wildtype mice (Figure 4d). No data were generated for the corpus or cauda epididymides, as tubules in these regions are extremely large and often seen in tangential or oblique section making it difficult to find sufficient transverse sections to perform quantitative analyses.

Light and electron microscopic analyses of morphological defects in Cst8$^{-/-}$ mice Testis

An examination of the testis of both the 4 and 10–12 month old *Cst8*$^{-/-}$ mice was performed by light microscopy and compared to that of wildtype mice. The testis of 4 month old *Cst8*$^{-/-}$ mice did not appear to be adversely affected compared to wildtype mice (data not shown). Many seminiferous tubules in older *Cst8*$^{-/-}$ mice also appeared normal and comparable to wildtype (Figure 5a), but there were others that appeared severely altered. These changes included sloughing of immature germ cells into the lumen of the seminiferous tubule (Figure 5b), separation of germ cells at the basal/adluminal junction of the epithelium (Figure 5c), and clumped and disoriented arrangement of late elongating spermatids relative to the lumen (Figure 5c). Some tubules failed to show a distinct lumen (Figures 5b,c).

By electron microscopy, some tubules in 10–12 month old Cst8$^{-/-}$ mice showed pyknotic nuclei of degenerating spermatocytes (Figure 5d). Some Sertoli cells also appeared to be degenerating as suggested by their deeply stained cytoplasm, highly dilated ER and absence of other characteristic organelles (Figure 5d). In some tubules, Sertoli cell processes did not have typical ectoplasmic specializations associated with clusters of elongating spermatids (Figure 5e). The ER cisternae hovering over the heads of late spermatids were greatly dilated (Figures 5e, 6b) and not flattened as seen in WT mice (Figure 6a), as were ER cisternae in the surrounding Sertoli cell cytoplasm (Figure 5e). In addition, the layer of filaments associated with ectoplasmic specializations in *Cst8*$^{-/-}$ mice appeared thinner and more inconspicuous (Figures 5e, 6b) compared to WT mice (Figure 6a). In some tubules, the base of the seminiferous epithelium was highly disrupted with large spaces between germ cells. Occupying these spaces were numerous cross sectional profiles of Sertoli cell processes not associated with germ cells. Some late spermatids appeared disoriented, and while embedded deep within the epithelium, they were enveloped by thin Sertoli cell processes (Figure 6c). Ectoplasmic specializations of Sertoli cells were poorly developed in association with these cells (Figure 6c). In some tubules, elongating spermatids had acrosomes that were highly dilated, irregular in shape and pale stained, and the accompanying ectoplasmic specialization showed disarrayed arrangements of filaments and dilated overlying ER cisternae (Figure 6c inset). The testes of 4 month old *Cst8*$^{-/-}$ mice were also examined by electron microscopy but the abnormalities observed in the older mice were not detected (data not shown).

Efferent ducts

The epithelial cells of the efferent ducts appeared unaffected in 4 and 10–12 month old *Cst8*$^{-/-}$ mice compared to wildtype mice. These cells maintained their high endocytic nature without apparent alterations to endosomes, multivesicular bodies (MVBs) or lysosomes (data not shown).

Epididymis

By light microscopy, the epididymis in 10–12 month old *Cst8*$^{-/-}$ mice exhibited large dense bodies that were prominent in the supranuclear region of the principal cells in the proximal initial segment (Figure 7a) as well as in all other regions. Immature germ cells were also noted in the lumen. Similar abnormalities were also noted by light microscopy in the epididymides of 4 month old *Cst8*$^{-/-}$ mice but these were much less pronounced than in the older mice (data not shown).

By electron microscopy, the principal cells of wild type mice showed a large supranuclear Golgi apparatus, abundant ER cisternae and a well developed endocytic apparatus consisting of endosomes, MVBs and lysosomes. The latter were small in size, more or less spherical and dense staining (Figure 7b). While many of the organelles in principal cells of 10–12 month old *Cst8*$^{-/-}$ mice appeared normal, principal cells in the initial segment and caput showed many large, dense, amorphous supranuclear bodies (Figure 7c). At higher magnification, such bodies were enveloped by a unit membrane and contained many irregular structures of different shapes (globular/tubular/spherical/beaded) and sizes. The enclosed structures were embedded in a moderately stained homogeneous granular matrix (Figure 7d–f). Similar structures were also seen in principal cells in the corpus and cauda, however, they were abundant basally as well as supranuclearly and often looked empty except for whorls of dense membranous material (Figure 8a,b). In all epididymal regions, such structures were identified as lysosomes due to their immunoreactivity with an anti-prosaposin antibody (Figure 8b inset), a marker for lysosomes in normal principal cells along the entire epididymis (Hermo et al, 1992a). In the cauda epididymidis, some clear cells also showed pleomorphic lysosomes, although they were not found in any abundance (data not shown).

Electron Microscopic analysis of the epididymal lumen in Cst8−/− mice

Along with epithelial abnormalities, there were numerous luminal abnormalities, especially in the cauda region of 10–12 month old *Cst8*$^{-/-}$ mice. These included an abundance of immature germ cells in the lumen consistent with premature sloughing of cells from the seminiferous epithelium (Figures 7a, 9a,b). There were also abnormalities with spermatozoa which had kinked or bent tails, as evidenced by the presence of multiple cross sections of tails enveloped within a common cytoplasm (Figure 9c). The heads of spermatozoa showed irregularities in shape, and apparent lack or deformation of the acrosome (Figure 9b,c). Moreover, there were masses of amorphous non-membrane bound material that were often closely associated with or surrounded spermatozoa and their tails (Figures 9b,c). Such aggregates appeared to be of two different staining intensities, one moderately dense and the other more pale (Figures 9b,c). Such aggregates were highly conspicuous in older *Cst8*$^{-/-}$ mice.

Discussion

LM immunolocalization of CRES in the testis, efferent ducts and epididymis

Our data on CRES distribution in testis confirms it is present exclusively in spermatids where the protein first appears in step 7 spermatids, peaks at step 12 and remains in high amounts until spermiation at step 16. This localization pattern is identical in either zinc or

Bouin's-fixed testes, and is consistent with previous reports of CRES distribution in the testis (Cornwall et al, 1992; Cornwall and Hann, 1995). Previous studies have reported that CRES localizes to the acrosome of isolated mouse and human spermatozoa (Syntin and Cornwall, 1999; Wassler et al, 2002), but we obtained no evidence of acrosomal staining in spermatozoa in tissues of mice or rats using our two methods of fixation and immunolocalization. The dissimilarity between the two studies may reflect differences in the procedures used for the preparation and/or fixation of the samples. In addition, we noted that residual bodies were CRES-positive after detaching from elongating spermatids at the time of spermiation, suggesting a role for CRES in these structures; the degree of residual body staining appeared to correlate with their state of degradation. Moreover, we did not detect CRES in cytoplasmic droplets that remain attached to sperm released into the tubular lumen, reflecting the capacity of these structures to be highly selective regarding what they contain. Indeed as residual bodies form at step 16, most of the organelles (mitochondria, ribosomes, ER, lipid) of the elongating spermatid are incorporated into this structure. However, isolated Golgi saccular elements of the spermatid cytoplasm do not enter the residual body but are distinct components of the droplet (Oko et al, 1993), along with other proteins (Veri et al, 1994; Papp et al, 1995; Janulis et al, 1996). The absence of CRES suggests that it has no function in relation to the cytoplasmic droplet.

As reported in previous studies (Cornwall and Hann, 1995), CRES expression in spermatids appears to be cytoplasmic, suggesting an intracellular role for CRES in these cells. While an isoform of CRES which lacks a signal peptide has been suggested to be present in spermatids (Cornwall et al, 1999), confirmation of this remains to be verified and for which a function would have to be defined. Alternatively spermatids, in addition to production of the acrosome by the Golgi apparatus (Susi and Clermont, 1970; Susi et al, 1971; Hermo et al, 1980; Clermont et al, 1993; Hermo et al, 2010), also take up radioactive sugars and incorporate them into glycoproteins that are transported from the Golgi apparatus to the spermatid surface (Clermont and Tang, 1985), where some may be secreted. Thus, at present, in the absence of EM immunocytochemical data, a major hurdle, we cannot determine with any degree of certainty whether CRES is secreted into the lumen or plays a role intracellularly, but studies on this are being carried out at present.

The presence of CRES in apical vesicles of nonciliated cells of the efferent ducts presumably corresponds to its localization in endosomes known to fill the apical cytoplasm (Hermo and Morales, 1984; Hermo et al, 1988b; Hermo et al, 1994; Hess, 2002). Several testis-derived proteins synthesized by Sertoli cells are secreted into the lumen of seminiferous tubules and are taken up by the nonciliated cells, where a distinct reaction appears over apical endosomes (Hermo et al, 1991; Hermo et al, 1992a). Since nonciliated cells are mainly involved in endocytosis via a plethora of apical tubular coated pits, the immunoreaction in endosomes may correspond to CRES' internalization from the lumen and origin from the testis, suggesting secretion of CRES by spermatids. However, an RT-PCR product corresponding to *Cst8* mRNA was detected in efferent ducts of the rat (data not shown), suggesting that synthesis of CRES may occur in situ with possible secretion into the lumen. Although the nonciliated cells are not known for high levels of secretion, CRES may be secreted to perform its role in the lumen as spermatozoa pass through this duct en route to the epididymis. Our RT-PCR results are contradictory to earlier studies where CRES mRNA expression in mouse efferent ducts was not detected by in situ hybridization (Cornwall et al, 1992; Cornwall and Hann, 1995). This discrepancy may reflect differences between the rat and mouse in the levels of *Cst8* mRNA and/or sensitivity of the methods used for RNA detection.

In the epididymis, CRES localizes almost exclusively to the proximal initial segment and in particular to principal cells, as was reported in earlier studies (Cornwall et al, 1992;

Cornwall and Hann, 1995). Western blot analyses have confirmed that CRES protein is present and synthesized locally within epididymal tissue (Cornwall and Hann, 1995; Sutton et al, 1999; Syntin and Cornwall, 1999; Wassler et al, 2002). In addition, we found in this study that CRES localizes to the secretory apparatus of principal cells, in particular to the supranuclear Golgi apparatus and to the epididymal lumen, both suggestive of active luminal secretion. The intense apical expression of CRES in principal cells suggests localization in apical secretory granules which are prominent in these cells and which are distinct in size from endosomes (Hermo et al, 1991; Hermo et al, 1994)

From the distal initial segment towards the caput, principal cells become gradually less reactive and there is a change in the pattern of luminal reactions. Unlike the intense uniform reactivity seen in the proximal initial segment, large discrete highly reactive amorphous CRES aggregates become evident in the lumen of the distal epididymis, especially in the cauda region. While the specific nature of these aggregates is as yet undefined, our previous studies indicated that CRES has the propensity to self-aggregate and form amyloid structures (von Horsten et al., 2007). CRES has also been detected within the epididymal lumen in both SDS-sensitive and SDS-resistant high molecular mass complexes (von Horsten et al, 2007). Thus, it is possible that the amorphous aggregates represent CRES in an amyloid structure possibly in a complex with other proteins and these aggregates may carry out biological functions within the epididymal lumen. Other reports have described electron dense bodies in the epididymal lumen as containing the chaperones heat shock protein 1 (HSPD1) and tumor rejection antigen gp96 (TRA1) and proposed these structures could be multimolecular complexes that deliver proteins to the developing spermatozoa (Asquith et al., 2005). These structures were shown to be approximately the same average size (0.9 um) as the CRES aggregates (1 um). Thus one possibility is that CRES, in an organized matrix, may function as a structural component of these dense bodies.

Alternatively, aggregation may comprise a mechanism to control CRES function as a monomer or oligomer. Indeed, amyloid plaques in Alzheimer's disease have been proposed to be a mechanism to inactivate or sequester smaller soluble and potentially cytotoxic β-amyloid aggregates (Lansbury 1999; Shankar et al., 2008). Furthermore, cystatin C also self-aggregates and becomes inactive as a cysteine protease inhibitor following dimerization (Ekiel and Abrahamson, 1996). The formation of aggregates could inhibit monomeric/oligomeric CRES function until it is removed from the lumen by endocytosis as seems to occur by some clear cells in the cauda epididymides. Clear cells are highly endocytic (Moore and Bedford, 1979; Hermo et al, 1988a; Hermo et al, 1992b; Hermo and Robaire, 2002), and it would appear that CRES is internalized from the lumen and degraded within the numerous lysosomes present in these cells. Hence, clear cells may be involved in CRES turnover from the lumen of the cauda epididymides as has been noted for other proteins (Hermo et al, 1992b).

Characterization of Cst8$^{-/-}$ mice

There are modest but significant reductions in the size of testicular and epididymal tubules as well as ultrastructural alterations to these tissues in *Cst8*$^{-/-}$ mice. However most of the abnormalities in the *Cst8*$^{-/-}$ tissues were in aged (10–12 month old) mice and were not apparent in 4 month old mice indicating a cumulative effect of the loss of CRES. It is possible that the absence of CRES may create altered cellular conditions such as an altered epididymal luminal environment such that over time, the epididymal tissue becomes affected. Similarly in the testis, the loss of CRES may contribute to abnormal germ cell-Sertoli cell relationships that gradually become apparent with extended time. The fertility defect that we have recently described in the *Cst8*$^{-/-}$ spermatozoa (Chau and Cornwall, in press) likely does not represent a direct effect of the ultrastructural alterations noted in this report since mice 3–5 months of age were used in these studies and they were of an age in

which little to no testicular or epididymal ultrastructural abnormalities were observed. Indeed, light microscopic analysis of isolated spermatozoa from 3–5 month old *Cst8*$^{+/+}$ and *Cst8*$^{-/-}$ mice revealed no morphological differences (data not shown). We have not examined the fertility of aged mice to determine whether there are additional fertility defects to that observed in the younger mice.

In the testis of aged mice, the reductions in the tubule size appear to be caused primarily by premature release and degeneration of immature germ cells. The vacuolated seminiferous epithelium also is suggestive of germ cell loss as noted in this study. In addition, some spermatids in the testis and spermatozoa in the epididymal lumen of *Cst8*$^{-/-}$ mice have irregularly shaped heads, tail malformations and abnormally developed acrosomes. The sperm abnormalities were seen in both the proximal and distal regions of the epididymis. Because of the large cauda lumen, the abnormalities become more prominent. In addition, alterations in the overall shape and appearance of some Sertoli cells and release of immature germ cells into the lumen implicate CRES in maintenance of proper Sertoli-spermatid associations. It has been suggested that proteases and their corresponding inhibitors work synergistically and are involved in the adherence of germ cells to Sertoli cells and subsequent formation of intercellular junctions (Charron and Wright, 2005; Wong and Cheng, 2005). These data are consistent with early findings that protease-sensitive elements of unknown nature hold spermatids and Sertoli cells together (Russell, 1980). Hence CRES along with proteases may be involved in proper maintenance of ectoplasmic specializations, known to be involved in adhesions (Vogl et al, 1993; Russell, 1993) and which are abnormal in C*st8*$^{-/-}$ mice. In the absence of CRES, adhesions between Sertoli and germ cells are disrupted leading to disoriented Sertoli cell processes and release of immature germ cells into the lumen.

In the present study, lysosomes of principal cells throughout the entire epididymis of aged *Cst8*$^{-/-}$ mice appear as enlarged, irregularly shaped pleomorphic structures unlike the small spherical dense and prosaposin-positive lysosomes seen in wild type mice of the same age (Abou-Haila and Fain-Maurel, 1984; Hermo et al, 1992a). Such abnormal lysosomes are found mainly in the supranuclear region of principal cells in proximal epididymal regions, but both supra- and infranuclearly in distal regions. In the distal epididymal regions the lysosomal abnormalities also appear distinct from those in the proximal regions by the predominance of electron lucent material. Why such differences are present are unknown but suggest that distal epididymal regions are more prone to abnormalities in the absence of CRES. Such alterations are reminiscent of changes seen, albeit in a mild form, of a lysosomal storage disease. In some cases, the absence of a lysosomal enzyme results in the inability of internalized proteins or lipids to be properly degraded resulting in accumulation of these components and subsequent increase in the number and size of lysosomes (Neufeld et al, 1975; Hammel and Alroy, 1995; Zhou et al, 1995; Adamali et al, 1999; Korah et al, 2003). In *Cst8*$^{-/-}$ mice, the abnormal lysosomes suggest that either one or more resident lysosomal proteases, many of which are cysteine proteases, is/are being inhibited or that more material for disposal is entering into the lysosomes than can be digested and disposed of over the life span of principal cells. One possibility is that excess acrosin, a component of the acrosome of sperm (Meizel, 1972; Parrish and Polakoski, 1979; Castellani-Ceresa et al, 1983) is released from the abnormal spermatozoa in the epididymal lumen of the *Cst8*$^{-/-}$ mice leading to proteolysis of other luminal proteins and ultimately resulting in excessive material being taken up by the principal cells and ending up in their lysosomes. Alternatively, CRES structures within the lumen may directly affect other luminal proteins and their functions such the loss of CRES results in a perturbed luminal environment and subsequent uptake of luminal material.

It should be noted that clear cells of the epididymis do not exhibit a profound phenotype as seen in principal cells and this is also the case for nonciliated cells of the efferent ducts. Indeed, both nonciliated cells and clear cells are much more actively involved in endocytosis than principal cells, with both cell types containing a plethora of endosomes and lysosomes (Moore and Bedford, 1979; Hermo et al, 1984; Hermo et al, 1988a). Hence it is not unlikely that both of these cells would have ample amounts of lysosomal enzymes and turnover rates to tolerate the consequences arising from the loss of function of the *Cst8* gene.

Amorphous materials of two different electron densities were seen with high frequency in the epididymal lumen of *Cst8*$^{-/-}$ mice. While material of varying densities was not noted previously, these aggregates may correspond morphologically to the so called “death cocoons” described in the hamster epididymis by Olson et al (2004). These workers proposed that these entities represent a regulatory mechanism by which the epididymis rids itself of degenerating spermatozoa. This is consistent with our findings that many sperm in the older *Cst8*$^{-/-}$ mice have head and tail deformities and appear to be dying. Studies are in progress to determine if the amorphous material in the *Cst8*$^{-/-}$ mice is immunoreactive to an antibody against the fibrinogen-related protein fgl2, which was shown by Olson et al (2004) to be a component of the death cocoon material. Whether the death cocoon amorphous material is related to or distinct from the dense bodies described earlier is not known.

In summary, the loss of CRES has a significant impact on the structure and functions of the testis and epididymis. However, the observed pathologies were prevalent in aged but not in younger adult mice suggesting that the effects of the loss of CRES are cumulative. In the testis, CRES is important for maintenance of germ cell integrity and proper relationships with Sertoli cells. In the epididymis, CRES is important for maintenance of the proper structural integrity of its principal cells including their lysosomes as well as for maintenance of the luminal environment.

Acknowledgments

The technical assistance of Jeannie Mui was greatly appreciated.

References

Abou-Haila A, Fain-Maurel MA. Regional differences of the proximal part of mouse epididymis: morphological and histochemical characterization. Anat Rec. 1984; 209:197–208. [PubMed: 6465530]

Adamali HI, Somani IH, Huang JQ, Gravel RA, Trasler JM, Hermo L II. Characterization and development of the regional- and cellular-specific abnormalities in the epididymis of mice with beta-hexosaminidase A deficiency. J Androl. 1999; 20:803–24. [PubMed: 10591619]

Asquith KL, Harman AJ, McLaughlin EA, Nixon B, Aitken RJ. Localization and significance of molecular chaperones, heat shock protein 1, and tumor rejection antigen gp96 in the male reproductive tract and during capacitation and acrosome reaction. Biol Reprod. 2005; 72:328–337. [PubMed: 15456702]

Beckstead JH. A simple technique for preservation of fixation-sensitive antigens in paraffin-embedded tissues. J Histochem Cytochem. 1994; 42:1127–34. [PubMed: 8027531]

Benavides J, Garcia-Pariente C, Gelmetti D, Fuertes M, Ferreras MC, Garcia-Marin JF, Perez V. Effects of fixative type and fixation time on the detection of Maedi Visna virus by PCR and immunohistochemistry in paraffin-embedded ovine lung samples. J Virol Methods. 2006; 137:317–24. [PubMed: 16908077]

Castellani-Ceresa L, Berruti G, Colombo R. Immunocytochemical localization of acrosin in boar spermatozoa. J Exp Zool. 1983; 227:297–304. [PubMed: 6352853]

Charron, M.; Wright, WW. Proteases and protease inhibitors. In: Skinner, MK.; Griswold, MD., editors. Sertoli Cell Biology. London: Elsevier Academic Press; 2005. p. 121-152.

Clermont Y. Kinetics of spermatogenesis in mammals: seminiferous epithelium cycle and spermatogonial renewal. Physiol Rev. 1972; 52:198–236. [PubMed: 4621362]

Clermont, Y.; Oko, R.; Hermo, L. Cell Biology of Mammalian Spermatogenesis. In: Desjardin, C.; Ewing, L., editors. Cell and Molecular Biology of the Testis. New York/Oxford: Oxford University Press; 1993. p. 332-376.

Clermont Y, Tang XM. Glycoprotein synthesis in the Golgi apparatus of spermatids during spermiogenesis of the rat. Anat Rec. 1985; 213:33–43. [PubMed: 4073559]

Cornwall GA, Orgebin-Crist MC, Hann SR. The CRES gene: a unique testis-regulated gene related to the cystatin family is highly restricted in its expression to the proximal region of the mouse epididymis. Mol Endocrinol. 1992; 6:1653–64. [PubMed: 1280328]

Cornwall GA, Hann SR. Transient appearance of CRES protein during spermatogenesis and caput epididymal sperm maturation. Mol Reprod Dev. 1995; 41:37–46. [PubMed: 7619504]

Cornwall GA, Hsia N, Sutton HG. Structure, alternative splicing and chromosomal localization of the cystatin-related epididymal spermatogenic gene. Biochem J. 1999; 340:85–93. [PubMed: 10229662]

Cornwall, GA.; Lareyre, JJ.; Matusik, RJ.; Hinton, BT.; Orgebin-Crist, MC. Gene Expression and Epididymal Function. In: Robaire, B.; Hinton, BT., editors. The Epididymis: From Molecules to Clinical Practice. New York: Kluwer Academic/Plenum Publishers; 2002. p. 169-200.

Cornwall GA, Cameron A, Lindberg I, Hardy DM, Cormier N, Hsia N. The cystatin-related epididymal spermatogenic protein inhibits the serine protease prohormone convertase 2. Endocrinology. 2003; 144:901–8. [PubMed: 12586766]

Cornwall GA, Hsia N. A new subgroup of the family 2 cystatins. Mol Cell Endocrinol. 2003; 200:1–8. [PubMed: 12644294]

Cornwall GA, von Horsten HH, Swartz D, Johnson S, Chau K, Whelly S. Extracellular quality control in the spididymis. Asian J Androl. 2007; 9:500–7. [PubMed: 17589787]

Cornwall GA. New insights into epididymal biology and function. Hum Reprod Update. 2009; 15:213–27. [PubMed: 19136456]

Crabo B. Studies on the composition of epididymal content in bulls and boars. Acta Vet Scand. 1965; 22(SUPPL 5):1–94. [PubMed: 14311560]

De Kretser, DM.; Kerr, JB. The cytology of the testis. In: Knobil, E.; Neill, JD., editors. The Physiology of Reproduction. New York: Raven Press Ltd; 1988. p. 837-932.

Ekiel I, Abrahamson M. Folding-related dimerization of human cystatin C. J Biol Chem. 1996; 271:1314–21. [PubMed: 8576118]

Ghiso J, Jensson O, Frangione B. Amyloid fibrils in hereditary cerebral hemorrhage with amyloidosis of Icelandic type is a variant of gamma-trace basic protein (cystatin C). Proc Natl Acad Sci U S A. 1986; 83:2974–8. [PubMed: 3517880]

Haimov-Kochman R, Prus D, Ben-Chetrit E. Azoospermia due to testicular amyloidosis in a patient with familial Mediterranean fever. Hum Reprod. 2001; 16:1218–20. [PubMed: 11387295]

Hamilton, DW. Structure and function of the epithelium lining the ductuli efferentes, ductus epididymidis and ductus deferens in the rat. In: Greep, RO.; Astwood, EB., editors. Handbook of Physiology. Washington: American Physiological Society; 1975. p. 259-301.

Hammel I, Alroy J. The effect of lysosomal storage diseases on secretory cells: an ultrastructural study of pancreas as an example. J Submicrosc Cytol Pathol. 1995; 27:143–60. [PubMed: 7757942]

Hecht NB. Molecular mechanisms of male germ cell differentiation. Bioessays. 1998; 20:555–61. [PubMed: 9723004]

Hermo L, Rambourg A, Clermont Y. Three-dimensional architecture of the cortical region of the Golgi apparatus in rat spermatids. Am J Anat. 1980; 157:357–73. [PubMed: 7405873]

Hermo L, Morales C. Endocytosis in nonciliated epithelial cells of the ductuli efferentes in the rat. Am J Anat. 1984; 171:59–74. [PubMed: 6486069]

Hermo L, Dworkin J, Oko R. Role of epithelial clear cells of the rat epididymis in the disposal of the contents of cytoplasmic droplets detached from spermatozoa. Am J Anat. 1988; 183:107–24. [PubMed: 2849296]

Hermo L, Spier N, Nadler NJ. Role of apical tubules in endocytosis in nonciliated cells of the ductuli efferentes of the rat: a kinetic analysis. Am J Anat. 1988; 182:107–19. [PubMed: 3400619]

Hermo L, Wright J, Oko R, Morales CR. Role of epithelial cells of the male excurrent duct system of the rat in the endocytosis or secretion of sulfated glycoprotein-2 (clusterin). Biol Reprod. 1991; 44:1113–31. [PubMed: 1873386]

Hermo L, Morales C, Oko R. Immunocytochemical localization of sulfated glycoprotein-1 (SGP-1) and identification of its transcripts in epithelial cells of the extratesticular duct system of the rat. Anat Rec. 1992; 232:401–22. [PubMed: 1543265]

Hermo L, Oko R, Robaire B. Epithelial cells of the epididymis show regional variations with respect to the secretion of endocytosis of immobilin as revealed by light and electron microscope immunocytochemistry. Anat Rec. 1992; 232:202–20. [PubMed: 1546800]

Hermo L, Oko R, Morales CR. Secretion and endocytosis in the male reproductive tract: a role in sperm maturation. Int Rev Cytol. 1994; 154:106–89. [PubMed: 8083031]

Hermo, L.; Robaire, B. Epididymal Cell Types and their Functions. In: Robaire, B.; Hinton, BT., editors. The Epididymis: From Molecules to Clinical Practice. New York: Kluwer Academic/ Plenum Publishers; 2002. p. 81-102.

Hermo L, Schellenberg M, Liu LY, Dayanandan B, Zhang T, Mandato CA, Smith CE. Membrane domain specificity in the spatial distribution of aquaporins 5, 7, 9, and 11 in efferent ducts and epididymis of rats. J Histochem Cytochem. 2008; 56:1121–35. [PubMed: 18796408]

Hermo L, Pelletier RM, Cyr DG, Smith CE. Surfing the wave, cycle, life history, and genes/proteins ecpressed by testicular germ cells. Part 2: Changes in spermatid organelles asspciated with development of spermatozoa. Microsc Res Tech. 2010 in press.

Hess RA. Oestrogen in fluid transport in efferent ducts of the male reproductive tract. Rev Reprod. 2000; 5:84–92. [PubMed: 10864852]

Hess, RA. The Efferent Ductules: Structure and Functions. In: Robaire, B.; Hinton, BT., editors. The Epididymis: From Molecules to Clinical Practice. New York: Kluwer Academic/Plenum Publishers; 2002. p. 49-80.

Hsia N, Cornwall GA. Cres2 and Cres3: new members of the cystatin-related epididymal spermatogenic subgroup of family 2 cystatins. Endocrinology. 2003; 144:909–15. [PubMed: 12586767]

Hsia N, Brousal JP, Hann SR, Cornwall GA. Recapitulation of germ cell- and pituitary-specific expression with 1.6 kb of the cystatin-related epididymal spermatogenic (Cres) gene promotor in transgenic mice. J Androl. 2005; 26:249–57. [PubMed: 15713831]

Ilio KY, Hess RA. Structure and function of the ductuli efferentes: a review. Microsc Res Tech. 1994; 29:432–67. [PubMed: 7873793]

Janulis L, Hess RA, Bunick D, Nitta H, Janssen S, Asawa Y, Bahr JM. Mouse epididymal sperm contain active P450 aromatase which decreases as sperm traverse the epididymis. J Androl. 1996; 17:111–6. [PubMed: 8723434]

Kierszenbaum AL, Rivkin E, Tres LL. Molecular biology of sperm head shaping. Soc Reprod Fertil Suppl. 2007; 65:33–43. [PubMed: 17644953]

Korah N, Smith CE, D'Azzo A, Mui J, Hermo L. Characterization of cell- and region-specific abnormalities in the epididymis of cathepsin A deficient mice. Mol Reprod Dev. 2003; 66:358–73. [PubMed: 14579412]

Lansbury PT. Evolution of amyloid: What normal protein folding may tell us about fibrillogenesis and disease. Proc Natl Acad Sci. 1999; 96:3342–3344. [PubMed: 10097040]

Leblond CP, Clermont Y. Definition of the stages of the cycle of the seminiferous epithelium in the rat. Ann N Y Acad Sci. 1952; 55:548–73. [PubMed: 13139144]

Lykidis D, Van Noorden S, Armstrong A, Spencer-Dene B, Li J, Zhuang Z, Stamp GW. Novel zinc-based fixative for high quality DNA, RNA and protein analysis. Nucleic Acids Res. 2007; 35:e85. [PubMed: 17576663]

Meizel S. Biochemical detection and activation of an inactive form of a trypsin-like enzyme in rabbit testes. J Reprod Fertil. 1972; 31:459–62. [PubMed: 4648130]

Moore HD, Bedford JM. Short-term effects of androgen withdrawal on the structure of different epithelial cells in the rat epididymis. Anat Rec. 1979; 193:293–311. [PubMed: 426300]

Nagamori I, Sassone-Corsi P. The chromatoid body of male germ cells: epigenetic control and miRNA pathway. Cell Cycle. 2008; 7:3503–8. [PubMed: 19001854]

Neufeld EF, Lim TW, Shapiro LJ. Inherited disorders of lysosomal metabolism. Annu Rev Biochem. 1975; 44:357–76. [PubMed: 806251]

Nistal M, Santamaria L, Codesal J, Paniagua R. Secondary amyloidosis of the testis: an electron microscopic and histochemical study. Appl Pathol. 1989; 7:2–7. [PubMed: 2706140]

Oakberg EF. A description of spermiogenesis in the mouse and its use in analysis of the cycle of the seminiferous epithelium and germ cell renewal. Am J Anat. 1956; 99:391–414. [PubMed: 13402725]

Oko R, Hermo L, Chan PT, Fazel A, Bergeron JJ. The cytoplasmic droplet of rat epididymal spermatozoa contains saccular elements with Golgi characteristics. J Cell Biol. 1993; 123:809–21. [PubMed: 8227142]

Olson GE, Winfrey VP, NagDas SK, Melner MH. Region-specific expression and secretion of the fibrinogen-related protein, fgl2, by epithelial cells of the hamster epididymis and its role in disposal of defective spermatozoa. J Biol Chem. 2004; 279:51266–74. [PubMed: 15377663]

Orgebin-Crist, MC.; Danzo, BJ.; Davies, J. Endocrine control of the development and maintenance of sperm fertilizing ability in the epididymis. In: Greep, RO.; Astwood, EB., editors. Handbook of Physiology. Washington: American Physiological Society; 1975. p. 319-338.

Papp S, Robaire B, Hermo L. Immunocytochemical localization of the Ya, Yc, Yb1, and Yb2 subunits of glutathione S-transferases in the testis and epididymis of adult rats. Microsc Res Tech. 1995; 30:1–23. [PubMed: 7711317]

Parrish RF, Polakoski KL. Mammalian sperm proacrosin-acrosin system. Int J Biochem. 1979; 10:391–5. [PubMed: 383541]

Parvinen M. The chromatoid body in spermatogenesis. Int J Androl. 2005; 28:189–201. [PubMed: 16048630]

Pennacchio LA, Lehesjoki AE, Stone NE, Willour VL, Virtaneva K, Miao J, D'Amato E, Ramirez L, Faham M, Koskiniemi M, Warrington JA, Norio R, de la Chapelle A, Cox DR, Myers RM. Mutations in the gene encoding cystatin B in progressive myoclonus epilepsy (EPM1). Science. 1996; 271:1731–4. [PubMed: 8596935]

Robaire, B.; Hermo, L. Efferent Ducts, Epididymis, and Vas Deferens: Structure, Functions, and Their Regulation. In: Knobil, E.; Neill, J., editors. The Physiology of Reproduction. 1. New York: Raven Press, Ltd; 1988. p. 999-1080.

Robaire, B.; Hinton, BT.; Orgebin-Crist, MC. The Epididymis. In: Neill, J., editor. Physiology of Reproduction. 3. San Diego: Elsevier Academic Press; 2006. p. 1071-1148.

Russell LD. Sertoli-germ cell interrelations: a review. Gamete Research. 1980; 3:179–202.

Russell, LD. Morphological and Functional Evidence for Sertoli-germ Cell Relationships. In: Russel, LD.; Griswold, MD., editors. The Sertoli Cell. Clearwater: Cache River Press; 1993. p. 365-390.

Shankar GM, Shaomin L, Mehta TH, Garcia-Munoz A, Shepardson NE, Smith I, Brett FM, Farrell MA, Rowan MJ, Lemere CA, Regan CM, Walsh DM, Sabatini BL, Selkoe D. Amyloid β-protein dimers isolated directly from Alzheimer brains impair synaptic plasticity and memory. Nat Med. 2008; 14:837–842. [PubMed: 18568035]

Susi FR, Clermont Y. Fine structural modifications of the rat chromatoid body during spermiogenesis. Am J Anat. 1970; 129:177–91. [PubMed: 4097414]

Susi FR, Leblond CP, Clermont Y. Changes in the golgi apparatus during spermiogenesis in the rat. Am J Anat. 1971; 130:251–67. [PubMed: 4101823]

Sutton HG, Fusco A, Cornwall GA. Cystatin-related epididymal spermatogenic protein colocalizes with luteinizing hormone-beta protein in mouse anterior pituitary gonadotropes. Endocrinology. 1999; 140:2721–32. [PubMed: 10342863]

Sutton-Walsh HG, Whelly S, Cornwall GA. Differential effects of GnRH and androgens on Cres mRNA and protein in male mouse anterior pituitary gonadotropes. J Androl. 2006; 27:802–15. [PubMed: 16837735]

Syntin P, Cornwall GA. Immunolocalization of CRES (Cystatin-related epididymal spermatogenic) protein in the acrosomes of mouse spermatozoa. Biol Reprod. 1999; 60:1542–52. [PubMed: 10330117]

Veri JP, Hermo L, Robaire B. Immunocytochemical localization of glutathione S-transferase Yo subunit in the rat testis and epididymis. J Androl. 1994; 15:415–34. [PubMed: 7860422]

Vogl, AW.; Pfeiffer, DC.; Redenbach, DM.; Grove, BD. Sertoli Cell Cytoskeleton. In: Russell, LD.; Griswold, MD., editors. The Sertoli Cell. Clearwater: Cache River Press; 1993. p. 39-86.

von Horsten HH, Johnson SS, SanFrancisco SK, Hastert MC, Whelly SM, Cornwall GA. Oligomerization and transglutaminase cross-linking of the cystatin CRES in the mouse epididymal lumen: potential mechanism of extracellular quality control. J Biol Chem. 2007; 282:32912–23. [PubMed: 17855342]

Wassler M, Syntin P, Sutton-Walsh HG, Hsia N, Hardy DM, Cornwall GA. Identification and characterization of cystatin-related epididymal spermatogenic protein in human spermatozoa: localization in the equatorial segment. Biol Reprod. 2002; 67:795–803. [PubMed: 12193387]

Wing T-Y, Christensen KA. Morphometric Studies on Rat Seminiferous Tubules. The American Journal of Anatomy. 1982; 165:13–25. [PubMed: 7137056]

Wong CH, Cheng CY. The blood-testis barrier: its biology, regulation, and physiological role in spermatogenesis. Current Topics in Developmental Biology. 2005; 71:263–296. [PubMed: 16344108]

Zeeuwen PL, van Vlijmen-Willems IM, Olthuis D, Johansen HT, Hitomi K, Hara-Nishimura I, Powers JC, James KE, op den Camp HJ, Lemmens R, Schalkwijk J. Evidence that unrestricted legumain activity is involved in disturbed epidermal cornification in cystatin M/E deficient mice. Hum Mol Genet. 2004; 13:1069–79. [PubMed: 15044380]

Zhou XY, Morreau H, Rottier R, Davis D, Bonten E, Gillemans N, Wenger D, Grosveld FG, Doherty P, Suzuki K, Grosveld GC, d'Azzo A. Mouse model for the lysosomal disorder galactosialidosis and correction of the phenotype with overexpressing erythroid precursor cells. Genes Dev. 1995; 9:2623–34. [PubMed: 7590240]

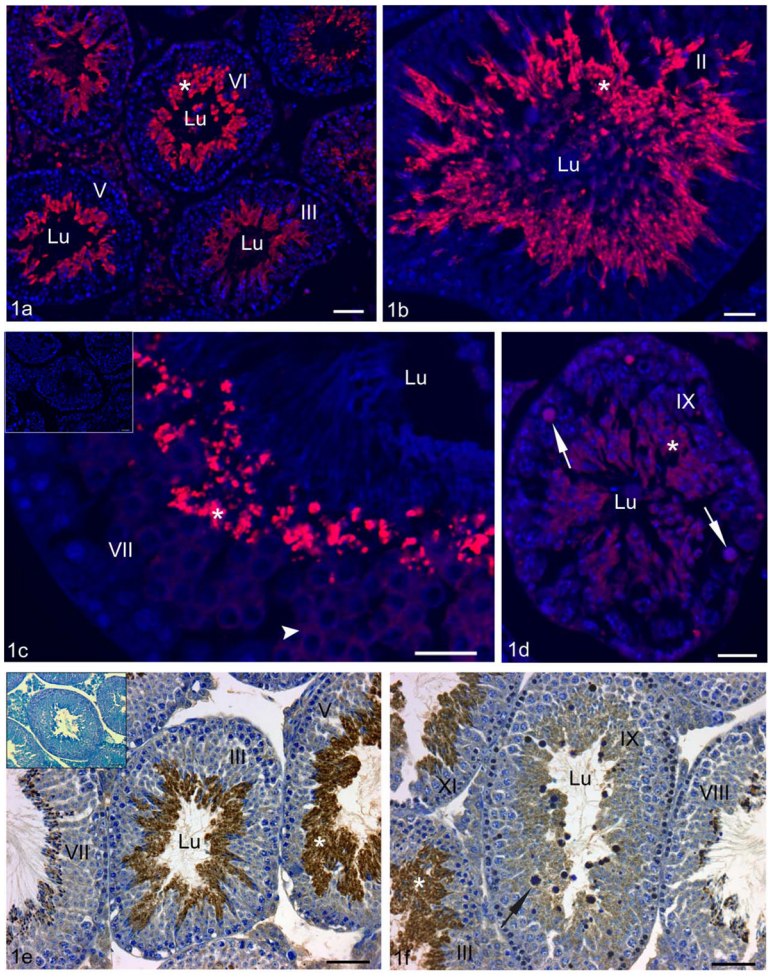

Figure 1.

Adult C57Bl/6 mouse testis fixed either with zinc fixative and visualized using immunofluorescence (a–d) or with Bouin's fixative and processed by DAB immunoperoxidase methods (e–f) and incubated with anti-CRES antibody. At low magnification (a), several seminiferous tubules at different stages of the cycle are evident revealing localization of CRES to spermatids (asterisk) in the adluminal compartment. At higher magnification, CRES immunoreactions (asterisks) are intense in step 14 elongating spermatids at stage II (b), as well as in step 16 spermatids at stage VII (c). CRES immunoreactivity first appears in step 7 spermatids (c) which show a weak to moderate immunostaining (c, arrowhead). Seminiferous tubules at stage IX (d) show a moderate reaction in step 9 spermatids (asterisk) which persists in residual bodies (arrows). In (e and f), several tubules at low magnification show no apparent reaction over spermatogonia and spermatocytes, while immunoreactions for CRES are intense over the cytoplasm of step 11 spermatids at stage XI, step 14 spermatids at stage III and step 15 spermatids at stage V (asterisk). In (f), at stage IX of the cycle, step 9 spermatids are moderately stained and residual bodies (arrow) reveal a rim of reactivity around their methylene blue stained core. Inset (c), negative control performed in the absence of anti-CRES antibody shows no reaction. Inset (e), negative control performed with CRES antibody preincubated with CRES protein revealed no reaction over the seminiferous epithelium confirming antibody specificity. Bars: a,e,e inset, f = 50 μm; b,c,c inset, d = 25 μm.

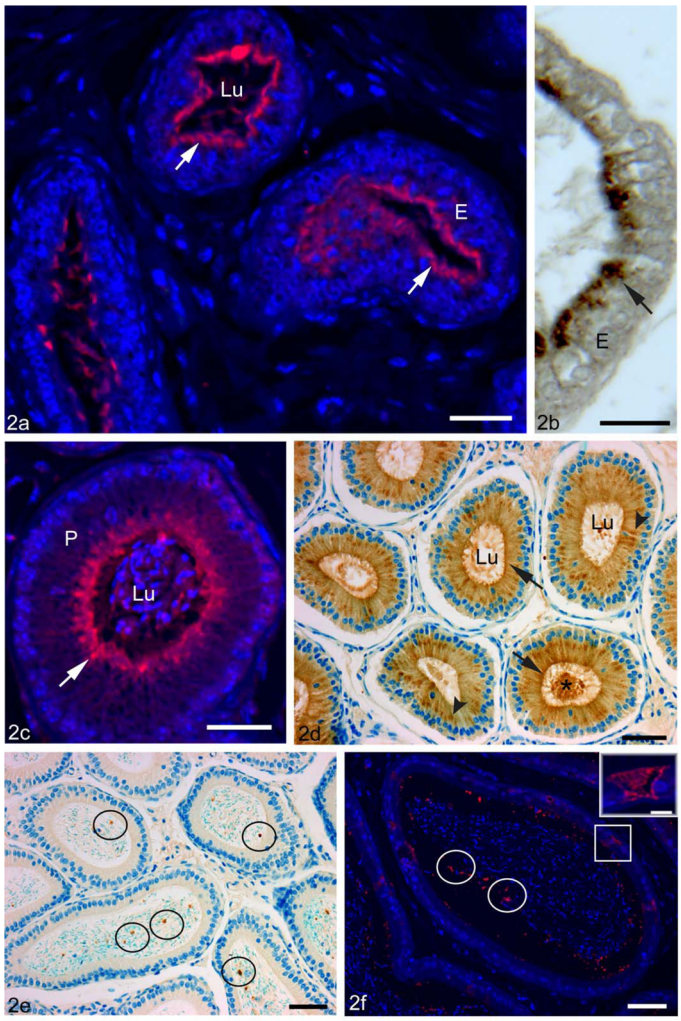

Figure 2.

Adult C57Bl/6 mouse efferent ducts (a,b) and epididymis (c–f) fixed with zinc fixative, incubated with anti-CRES antibody and visualized by immunofluorescence (a,c,f) or fixed with Bouin's fixative and stained by DAB immunoperoxidase methods (b,d,e). In the efferent ducts (a), several tubules show uniform reactions over the apical region (arrows) of the epithelium (E). At high magnification, the epithelial cells (E) show a vesiculated reaction in their apical cytoplasm (arrow) (b). In the proximal initial segment of the epididymis (c,d), CRES immunoreactions are prominent in the apical region of principal cells (P) where it appears as diffuse staining with several hot spots (arrows), while in (d), a prominent supranuclear reaction corresponding to the Golgi apparatus is also noted (arrowheads). In (c,d), intense staining also appears in the lumen (Lu, asterisk). Epithelium in the caput (e) and cauda (f) show no obvious immunoreactivity for CRES; however, a few focal aggregates of intense reactivity are randomly distributed in the lumen (circles). Sperm show no apparent reactivity in the caput (e) or cauda (f). Some highly endocytic clear cells (squares) show strong immunostaining for CRES in the cauda region (f). Inset of (f): a high magnification of a reactive clear cell. Bars: a,c = 25 μm; d,e,f = 50 μm; b = 20 μm; f inset = 10 μm.

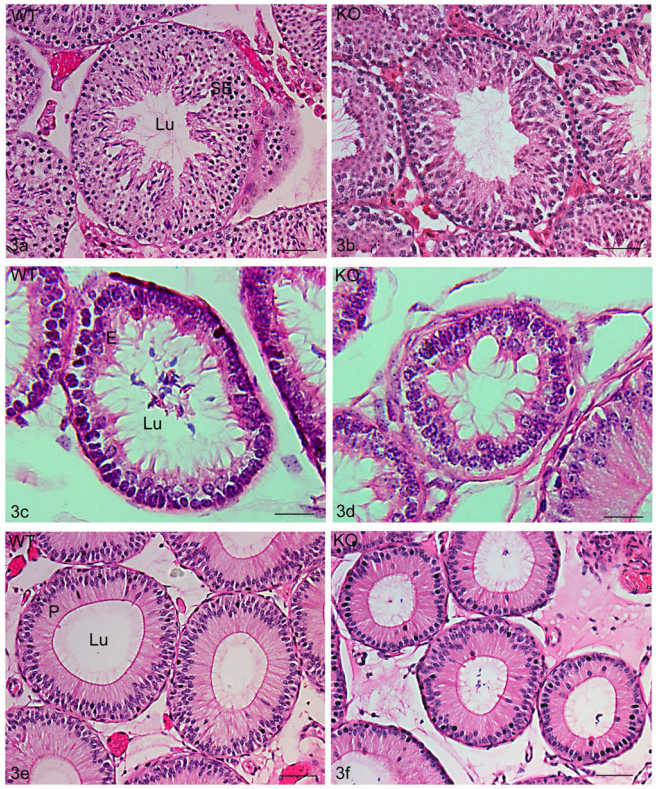

Figure 3.

Hematoxylin and eosin stained adult testis (a,b), efferent ducts (c,d) and proximal initial segment (e, f) of 10–12 month old wildtype (WT, *Cst8*$^{+/+}$) (a,c,e) and knockout (KO, *Cst8*$^{-/-}$)(b,d,f) mice. Tubules in *Cst8*$^{-/-}$ mice were consistently smaller compared to WT. SE, seminiferous epithelium; Lu, lumen. Bars: a,b,e,f = 50 μm; c,d = 20 μm.

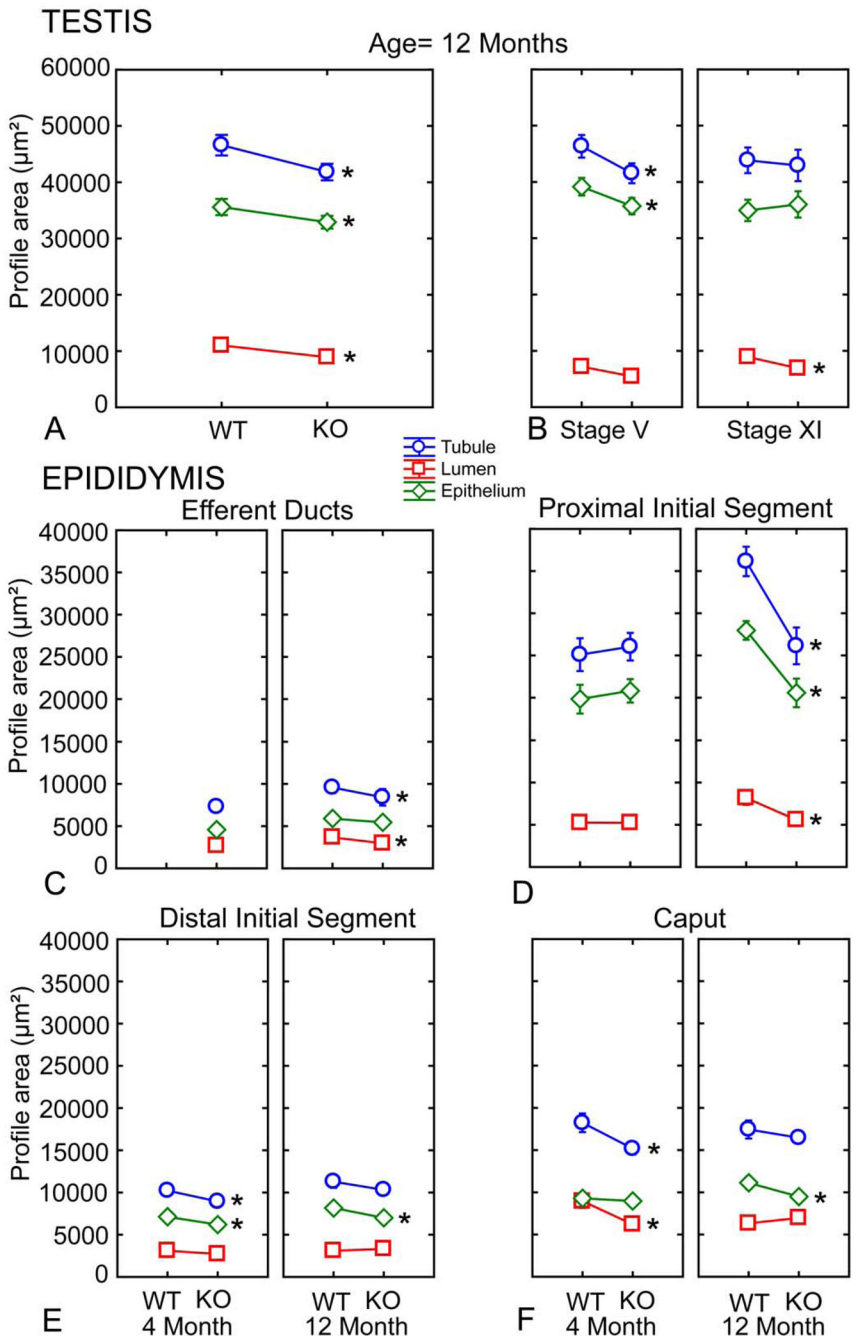

Figure 4.

Morphometric data on profile area measurements in the epithelium, lumen and tubule obtained from the testis, efferent ducts and epididymis of WT (*Cst8*$^{+/+}$) and KO (*Cst8*$^{-/-}$) mice at 4 and 10–12 months of age. Tubular, epithelial and luminal areas were collected from eighty (testis) or forty (epididymis) tubules in each subgroup of the data set. A) Seminiferous epithelium of the testis from mice aged 10–12 months; B) Stage specificity of the seminiferous epithelium from mice aged 10–12 months; C) Efferent ducts; D) Proximal initial segment; E) Distal initial segment; F) Caput. Circles (Tarea) indicate tubule profile area, diamonds (Earea) indicate epithelial profile area, and squares (Larea) indicate luminal profile area. Asterisks indicate difference of means that are significant ($p < 0.05$). The most

profound changes are seen in the proximal initial segment of the epididymis of older mice (d).

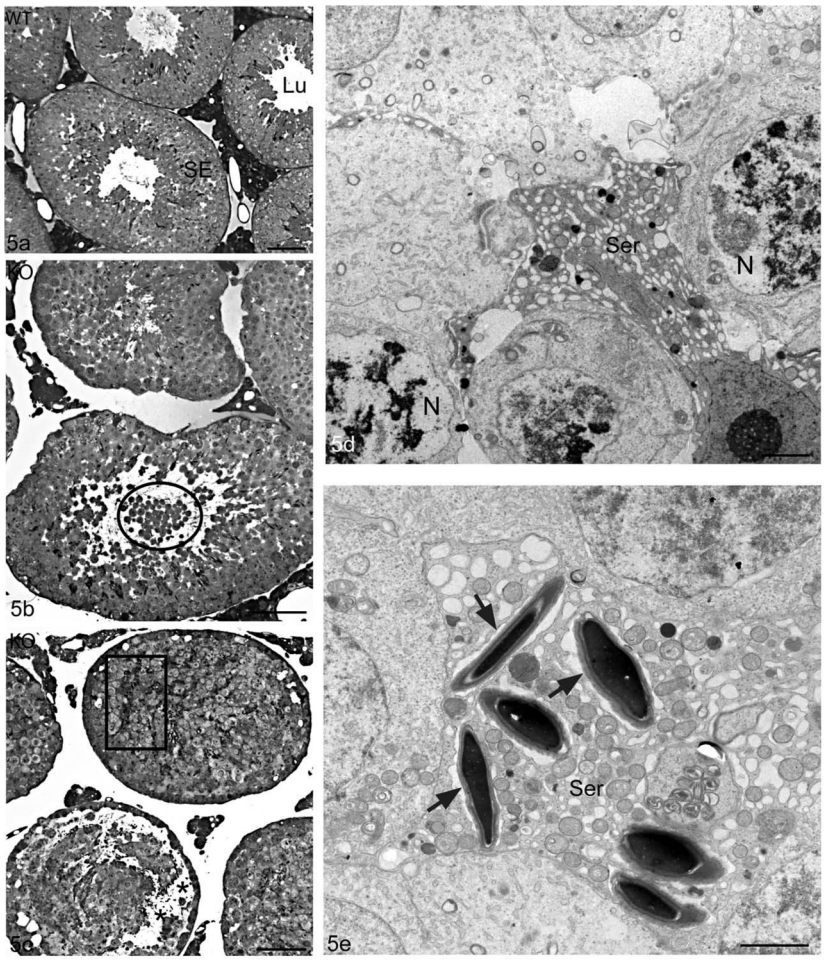

Figure 5.

Light micrographs of the seminiferous epithelium of WT (*Cst8*$^{+/+}$) (a) and KO(*Cst8*$^{-/-}$) (b,c) 10–12 month old mice. In comparison to the intact seminiferous epithelium and unobstructed tubular lumen of WT mice (a), *Cst8*$^{-/-}$ tubules show shedding of immature germ cells into the lumen (b, circle) and disoriented late spermatids (c, box). *Cst8*$^{-/-}$ mice also display vacuolization in the epithelium, closure of the tubule lumen (b) and detachment of germ cells at the junction of the basal/adluminal compartment (c, asterisks). Electron micrographs (d,e) of the seminiferous epithelium of *Cst8*$^{-/-}$ 10–12 month old mice. In (d), several germ cells adjacent to a Sertoli cell (Ser) show nuclei (N) with abnormal chromatin patterns and pale stained areas including membranous whorls, all suggestive of degeneration. In (e), several late elongating spermatids are closely enveloped by a Sertoli cell (Ser) and although they have an acrosome, they are not oriented properly and show no association with ectoplasmic specializations. An empty looking space is present surrounding these spermatids (arrows). Seminiferous epithelium, SE; Lumen, Lu. Bars: a,b,c = 50 μm; d,e = 2 μm.

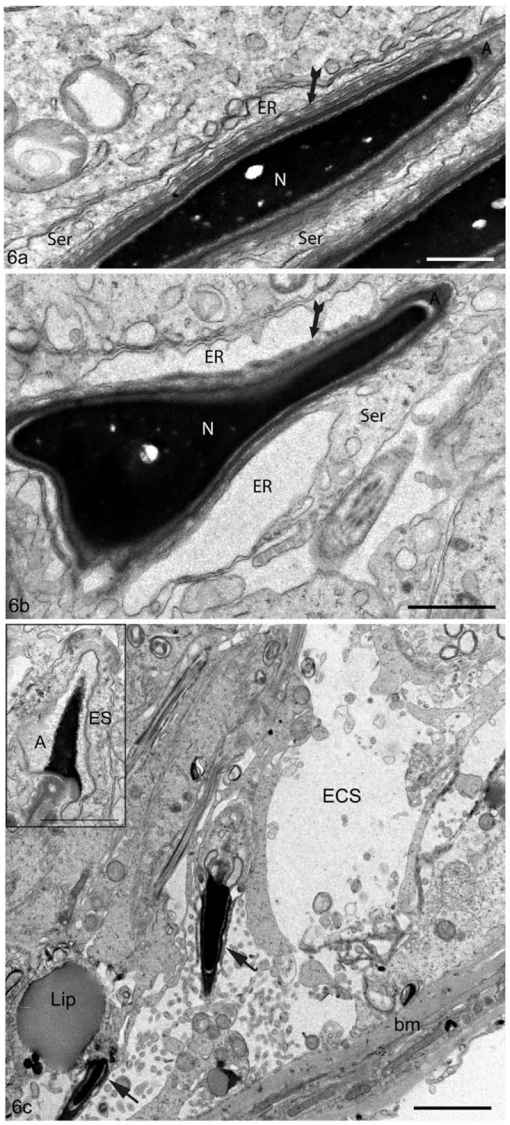

Figure 6.

Electron micrographs of the seminiferous epithelium of the testis of 10–12 month old WT (*Cst8*$^{+/+}$) (a) and KO (*Cst8*$^{-/-}$)(b,c) mice. In (a), the ectoplasmic specialization has bundles of filaments (fluted arrows) and a closely associated flattened cisterna of endoplasmic reticulum (ER). In (b), the ER appears highly dilated and the filament bundles (fluted arrows) are less conspicuous. In (c), the basal region of the epithelium appears to have lost germ cells resulting in an enlarged extracellular space (ECS). The large lipid droplet (Lip) is abnormal for this stage (II–III). Two elongating spermatids (arrows) are embedded deep in the seminiferous epithelium, and while they are associated with thin Sertoli cell processes, they do not display characteristic ectoplasmic specializations. Basement membrane, bm; Nucleus, N; Acrosome, A. Inset: the head of an elongating spermatid shows a dilated acrosome including an abnormal pale stained appearance and a disruption of the ectoplasmic specialization (ES). Bars: a = 0.5 μm; b,c inset = 1 μm; c = 2 μm.

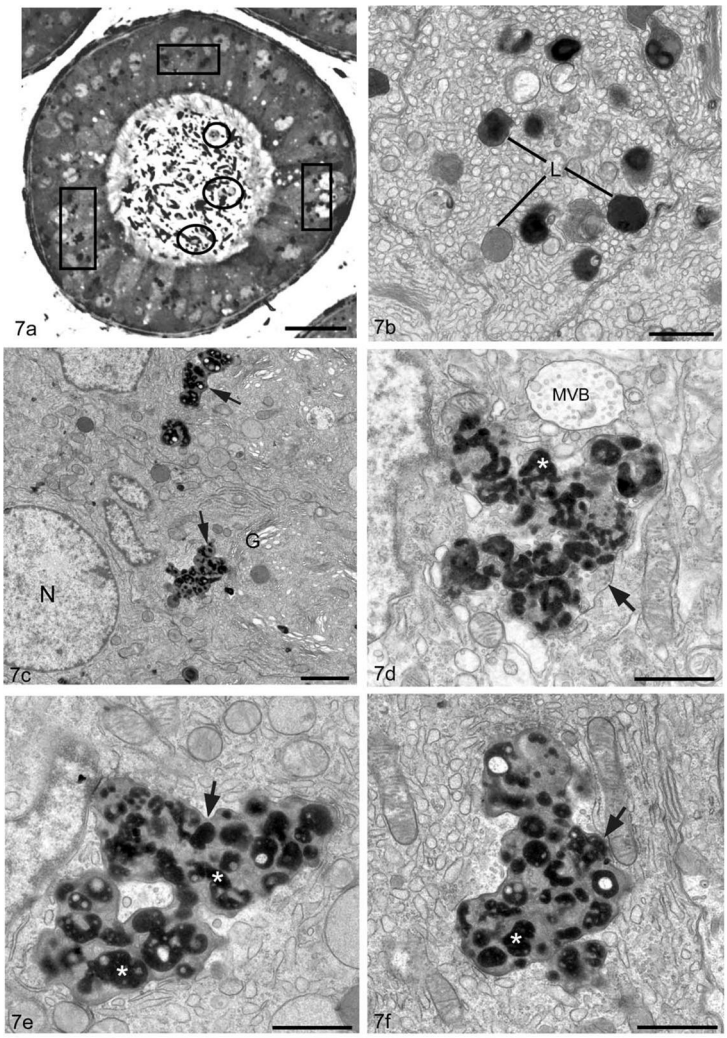

Figure 7.

Light micrograph (a) of a tubule of the proximal initial segment of a 10–12 month old *Cst8*$^{-/-}$ mouse displays large irregularly shaped supranuclear lysosomes (boxes) in principal cells and immature germ cells in the epididymal lumen (circles). Electron micrographs of the supranuclear region of principal cells of the initial segment of a WT (*Cst8*$^{+/+}$)(b) and KO (*Cst8*$^{-/-}$) (c–f) 10–12 month old mice. In WT (b), lysosomes (L) are small in size, more or less spherical and reveal dense granular whorls embedded in a moderately dense material or a homogeneous dense or moderately dense matrix. In KO (c–f), lysosomes (arrows) are extremely enlarged and pleomorphic in appearance. Surrounded by a unit membrane they contain numerous dense bodies (asterisk) with irregularly shapes and sizes in which paler areas are present; some dense bodies are at times spherical, bead-like or tubular in nature. Multivesicular body, MVB; nucleus, N; Golgi apparatus, G. Bars: a = 25 μm; b,d,e,f = 1 μm; c = 2 μm.

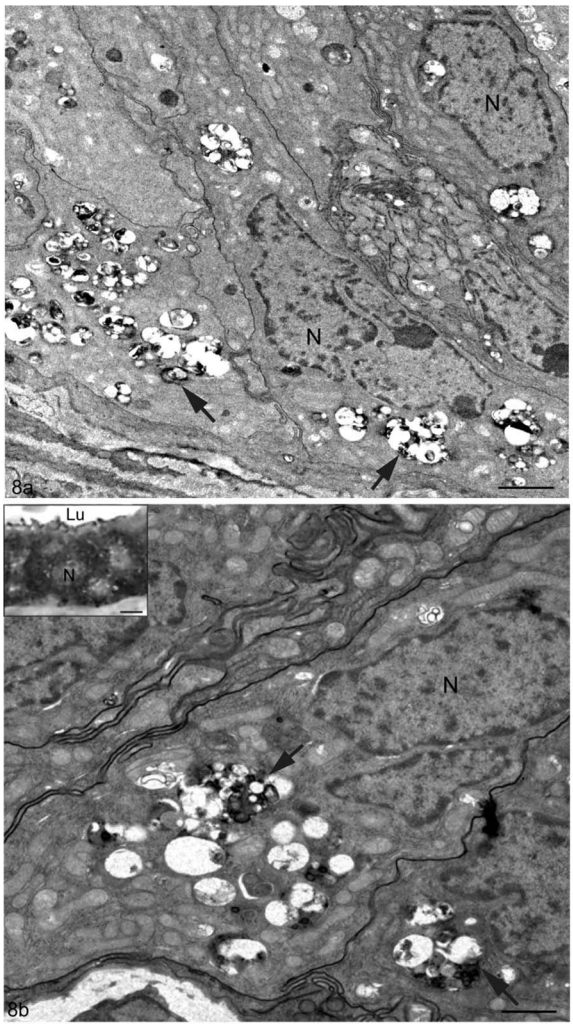

Figure 8.

Electron micrographs of the epithelium in the cauda of *Cst8*$^{-/-}$ mice at 10–12 months of age. In (a) and (b), principal cells reveal irregularities of their lysosomes (arrows), which appear numerous and irregularly shaped. They contain electron dense granular bodies of different shapes and sizes and membranous whorls, all embedded in an apparent electron lucent matrix. Such bodies are abundant and are situated both above and below the nucleus (N). Inset of (b) displays the epithelium of the proximal initial segment of a *Cst8*$^{-/-}$ mouse seen at the LM level immunostained with anti-prosaposin antibody. Principal cells show numerous reactive irregularly shaped large supranuclear lysosomes. Lumen, Lu. Bars: a, b = 2 μm; b inset = 5 μm.

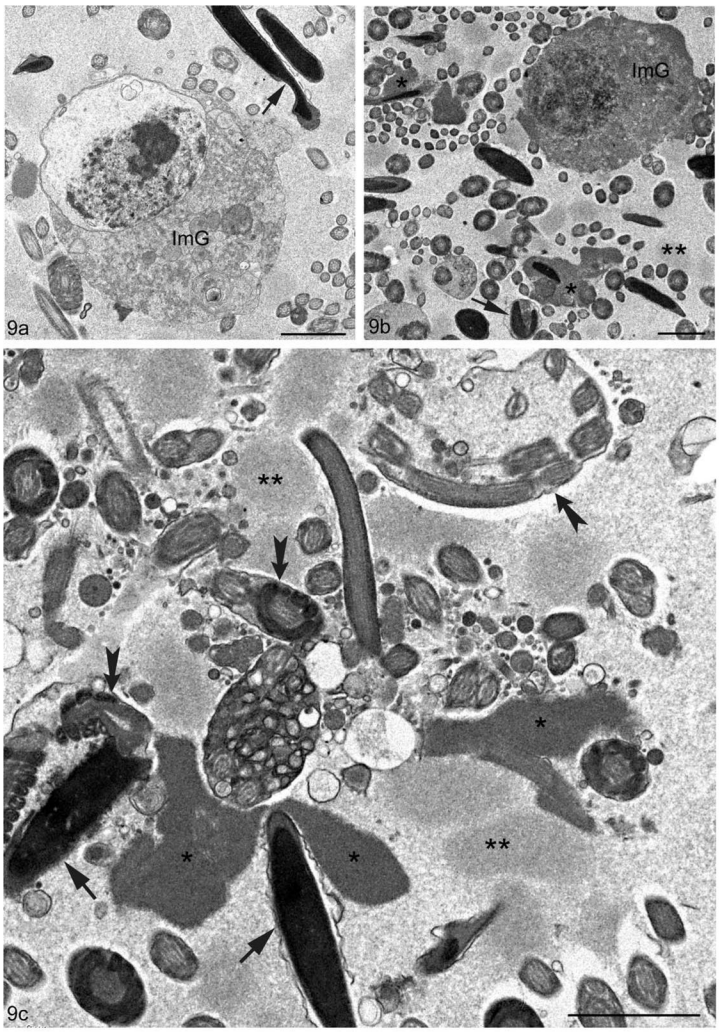

Figure 9.

Electron micrographs of the epididymal lumen in the cauda region of *Cst8*$^{-/-}$ mice at 10–12 months of age. In (a) and (b) immature spherical germ cells (ImG) are evident with a disrupted nucleus undergoing necrosis. Abnormal sperm heads are also indicated (arrow). In (b), the lumen shows the heads or tails of sperm in association with an amorphous material of uniform flocculent consistency with a dense (asterisks) or moderately dense (double asterisk) staining appearance. One sperm enveloped by a loose plasma membrane shows a bent head and absence of an acrosome (arrow). In (c), at higher magnification, the dense amorphous material (asterisks) and paler one (double asterisks) is prominent in the lumen and at times in association with sperm heads or tails. Some sperm heads appear abnormal with an incomplete acrosome (arrows). Tails of sperm are at times abnormal showing a bent nature, and often more than one cross sectional profile is evident enveloped in a common cytoplasm (fluted arrows). Bars: a–c = 2 μm.